Engineering Tribology and Materials

ICETAT 2016

Edited by
Yunn Lin Hwang and Jeng Haur Horng

TRANS TECH PUBLICATIONS

Engineering Tribology and Materials

ICETAT 2016

Edited by
Yunn Lin Hwang
Jeng Haur Horng

Engineering Tribology and Materials

ICETAT 2016

Selected, peer reviewed papers from the
International Conference on
Engineering Tribology and Applied Technology 2016
(ICETAT2016),
November 4-6, 2016, Taipei, Taiwan

Edited by

Yunn Lin Hwang and Jeng Haur Horng

Copyright © 2017 Trans Tech Publications Ltd, Switzerland

All rights reserved. No part of the contents of this publication may be reproduced or transmitted in any form or by any means without the written permission of the publisher.

Trans Tech Publications Ltd
Reinhardstrasse 18
8008 Zurich
Switzerland
http://www.scientific.net

Volume 739 of
Key Engineering Materials
ISSN print 1013-9826
ISSN cd 1662-9809
ISSN web 1662-9795

Full text available online at *http://www.scientific.net*

***Distributed** worldwide by*

Trans Tech Publications Ltd
Reinhardstrasse 18
8008 Zurich
Switzerland

Phone: +41 (44) 922 10 22
Fax: +41 (44) 922 10 33
e-mail: sales@scientific.net

and in the Americas by

Trans Tech Publications Inc.
PO Box 699, May Street
Enfield, NH 03748
USA

Phone: +1 (603) 632-7377
Fax: +1 (603) 632-5611
e-mail: sales-usa@scientific.net

Preface

This issue collected some selected tribology and materials research papers from the International Conference on Engineering Tribology and Applied Technology 2016 (ICETAT 2016). The conference had more than 150 scheduled papers and abstracts on the 2-day technical workshop sessions with several keynote lectures, 2-day poster sessions and exhibits. At the same time, the conference represented a unique opportunity for the tribology and engineering community to present their new research results, exchange ideas and become familiar with new trends and directions in the fields of Basic Friction and Wear, Biotribology, Computer-Aided Engineering, Contact Mechanics, Dynamic and Vibration Engineering, Green Tribology and Sustainability, Lubricants and Lubrication, Material Analysis and Examination, Manufacturing Technology, Measurement and Signal Processing Technology, Micro and Nano Tribology, Surface Engineering and Coating, Tribology in Machine Elements, etc. These papers including 3 plenary speech, 11 invited talks, 75 oral presentation and 65 poster papers on various topics which are presented in several parallel symposia in the conference. Consequently, ICETAT2016 provided an important platform for exchanging tribology and advanced engineering technologies.

We appreciated all the participants' contribution for submitting the excellent research works to the conference. At last, we would like to thank all the attendees for your participation. The papers presented in Journal of Key Engineering Materials were the selected manuscripts associated Tribology and Materials research areas from ICETAT2016. The other manuscripts associated engineering technology were published in the other profession journals.

Committee

Yunn-Lin Hwang, Jeng-Haur Horng

Sponsors

Ministry of Science and Technology (MOST)

Taiwan Society of Tribology Technology (TSTT)

National Formosa University (NFU)

Table of Contents

Key Engineering Materials
ISSN: 1662-9795, Vol. 739, pp 1-6
doi:10.4028/www.scientific.net/KEM.739.1
© 2017 Trans Tech Publications, Switzerland
Submitted: 2016-08-31
Accepted: 2017-03-12

Effect of Variation of Gap Thickness of the Thrust Bearing on Gap Pressure and Stiffness of the Aerostatic Spindle in Vertical Milling

Te-Yen Huang[1,a], Shi-Jie Weng[2,b], Shao-Yu Hsu[3,c]

[1]Department of Mechanical Engr, Lunghwa University of Sci. and Tech., Taoyuan, Taiwan

[2]Department of Mechanical Engr, National Taiwan University of Sci. and Tech., Taipei, Taiwan

[3]Mechanical and Systems Research Lab., Industrial Technology Research Inst., Hsinchu, Taiwan

[a]tyhuang@mail.lhu.edu.tw, [b]m10303326@mail.ntust.edu.tw, [c]shaoyuHsu@itri.org.tw

Keywords: Aerostatic spindle, Gap pressure, Journal bearing, Porous insert, Thrust bearing.

Abstract. When the partially porous aerostatic thrust bearing and the journal bearings of an aerostatic spindle in a vertical milling machine are subjected to cutting load and gravitational force, the thicknesses of gaps between the thrust plate and the spindle flange will change. This study applied CFD software to analyze the effect of variations of gap thickness and rotating speed on the pressure in the gaps of the bearings and the stiffness of the spindle. The results revealed that, when the thrust plate and the spindle flange were pushed back and forth by external loading, the pressure in the gap between the spindle flange and the thrust plate was affected significantly. The pressure in the gap between the spindle and the journal bearing was slightly affected. When the spindle rotated faster, the pressure on the surface of spindle became higher and the stiffness of spindle was increased.

Introduction

The porous aerostatic bearings are widely used in ultra precision machine tools. Due to good ability of the porous medium in flow restriction, the porous aerostatic bearings are better than other types of aerostatic bearings in characteristics such as load carrying capacity, stiffness, damping and dynamic stability in high speed. Many papers studying the fully porous aerostatic journal bearings have been published. However, research reports regarding the partially porous aerostatic journal bearing are rarely seen. So far, Szwarcman and Gorez [1] studied the aerostatic journal bearing with porous inserts to find the relationships for the load capacity, the stiffness and the gas flow rate of the bearing as functions of the supply pressure, the relative eccentricity and the geometry of the bearing. Rao [2] analyzed the characteristics of porous aerostatic journal bearing and verified the calculated results by experimental research. Wang [3] studied the effects of various parameters on characteristics of the partially porous aerostatic journal bearing. He proved the partially porous bearing was better than the fully porous bearing in terms of stiffness. Huang et al. [4] studied the effects of the size of porous medium, the bearing gap, the eccentricity and the spindle speed on the gap pressure, the load capacity and the stiffness of the fully porous and the partially porous aerostatic journal bearings.

During the feeding process, the spindle of a vertical milling machine is subjected to both axial and transverse compressive forces which cause a thinner air gap between the spindle flange and the rear thrust plate. During the retracting process, the dead weight of the spindle module results in a thinner air gap between the spindle flange and the front thrust plate. This paper studied how the changes in rotating speed and thicknesses of air gaps in the bearings affected the gap pressure and stiffness of spindle when the vertical milling machine was under machining operation.

Analytical Approach

Based on the finite volume method, this study utilized the laminar flow module of the CFD software, FLUENT, to solve the three dimensional Navier-Stokes equations to compute the pressure of air flow in the bearing gaps and the housing gaps in an aerostatic spindle. The k-ε equation for turbulence was used to analyze the physical parameters under the steady state condition. The second

order Upwind Differentiating Technique was adopted to solve the convection terms. In order to have optimum convergence and satisfactory accuracy, the pressure-velocity coupling scheme of the SIMPLEC approach was applied to solve the iterative equations to compute the velocity and the pressure. To simplify the simulation, the following assumptions were made for the flow field:

(1). The air was assumed to be a Newtonian flow with an invariant density. The effects of gravity, surface roughness and heat transfer were neglected.

(2). All physical properties were independent of the temperature. The ambient temperature was a constant. The properties of the porous material were isotropic and the porosity was a constant.

(3). Inside the porous material, the air flow obeyed the Darcy's law and was considered laminar due to its low velocity. And, the inertia resistance was neglected for the same reason.

The following boundary conditions were considered in analysis:

(1). On the inlet boundary, the air was pumped into the bearing at a gage pressure of 400 kPa. On the outlet boundary, the air was discharged to the ambient atmosphere at a gage pressure of 0 kPa.

(2).Wall function: The flow passing by the solid wall must meet not only the no-penetration condition, but also the no-slip condition. On selection of the standard $k-\varepsilon$ turbulent model, the standard wall function in the options of Near-Wall Treatment had to be employed.

(3) Slip wall: The surface of the porous material was assumed under slip wall boundary condition, the rest of solid surface was under no-slip condition.

(4). Moving wall: The moving wall boundary condition was defined for the surface of the spindle.

Simulation models

To reduce the size of the mesh, only the front portion of the aerostatic spindle module, as shown in Fig. 1, was considered in building the models for analysis. Fig. 2 illustrated the CAD model of the front part of the spindle module consisting of a partially porous aerostatic thrust bearing and a partially porous aerostatic journal bearing. There were eight porous inserts uniformly distributed on each of these two bearings. With a thickness of 3 mm and a diameter of 6 mm, each porous insert had a porosity of 0.2.

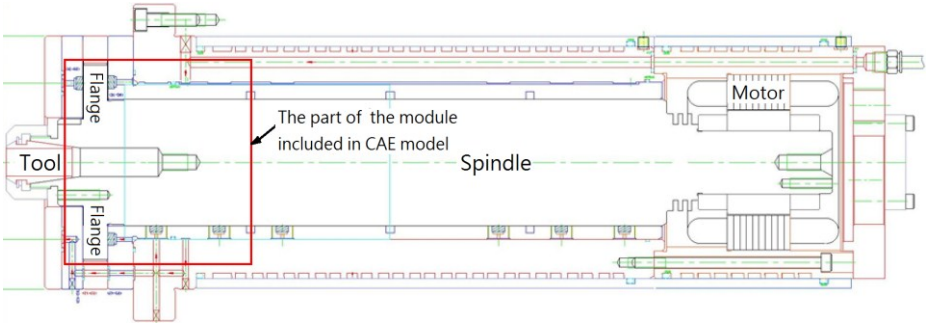

Fig. 1 The longitudinal section of the aerostatic spindle module. The front part of the module included in the CAE model is highlighted.

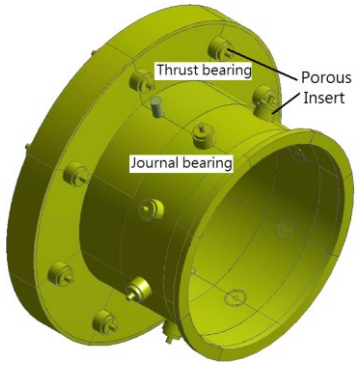

Fig. 2 The CAD model.

In the longitudinal section view of the model shown in Fig. 3(a), gap 3 was the air gap between the spindle flange beside the tool and the front thrust plate, gap 2 was the air gap between the spindle flange beside the journal bearing and the rear thrust plate, and gap 1 was the air gap between the spindle and the porous insert on the journal bearing or the air gap between the spindle and the housing. The axial line 1 located below gap 1, the radial lines 2 and 3 located at lower part of gaps 2 and 3 of the thrust bearing respectively. Fig. 3(b) showed the route of the air flow in the spindle module.

In the model, the outer diameter of the spindle was 60 mm, the inner diameter of the journal bearing was 60.02 mm. To avoid pressure drop, the thickness of the air gap between the spindle and the housing was kept the same as that between the spindle and the porous insert. Namely, the thickness of gap 1 was kept as 10 mm. In the initial stage (i.e., the feeding process) of vertical milling, when the cutting tool contacts the workpiece, it encounters cutting resistance in which axial

compressive force is dominant. Being pushed by this axial force, the thickness of air gap 2 between the spindle flange and the rear thrust plate was reduced from 10 μm to 7 μm. Thus, in the model for feeding process, the thicknesses of gap 2 and gap 3 were 7 μm and 13 μm respectively (Fig. 4(a)). When the cutting process has stabilized, the cutting force subjected to the spindle is mainly radial load. Thus, in the model for stabilized cutting process, both gap 2 and gap 3 were 10 μm in thickness (Fig. 4(b)). During retracting process, the thrust bearing was pushed by the dead weight of the spindle module, the thickness of air gap 3 between the spindle flange and the front thrust plate was reduced to 5 μm. Thus, in the model for retracting process, thicknesses of gap 2 and gap 3 were 15 μm and 5 μm respectively. (Fig. 4(c)). With an eccentricity ratio of 0.3, the pressure on the spindle and its stiffness were analyzed for a rotating speed of 15000 rpm, 30000 rpm and 60000 rpm respectively.

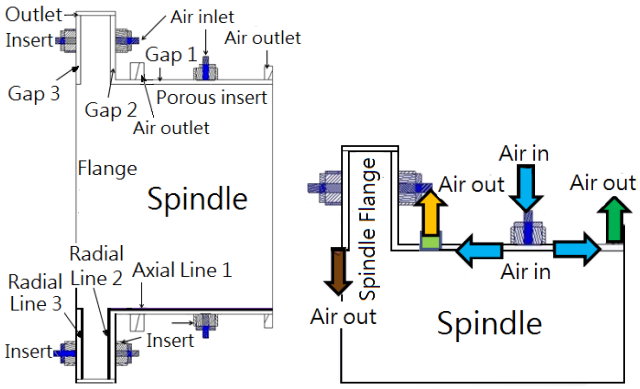

Fig. 3 (a) Logitudinal section view of spindle module. (b) Passage of air flow.

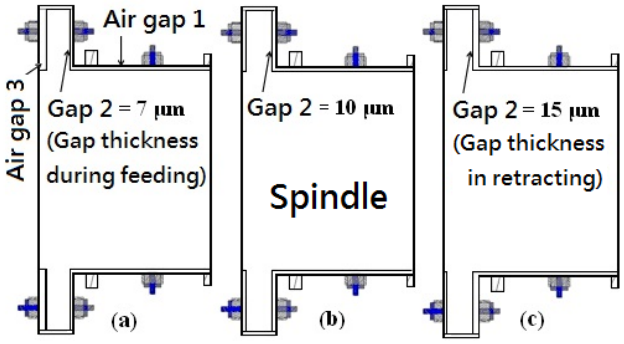

Fig. 4 Change in thickness of gap 2 during vertical milling operation.

Results and discussion

Variation of pressure in the air gap between the spindle and the journal bearing

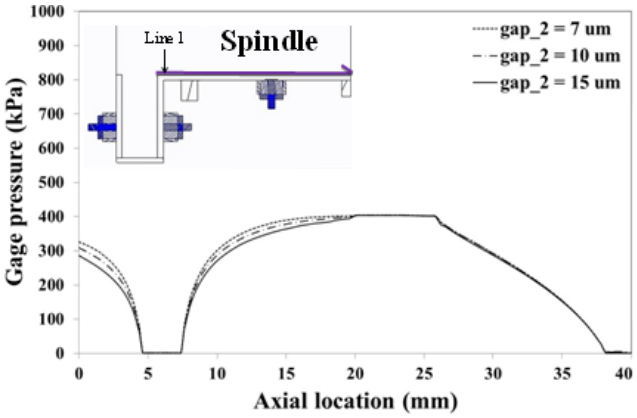

(a) Rotating speed = 15000 rpm

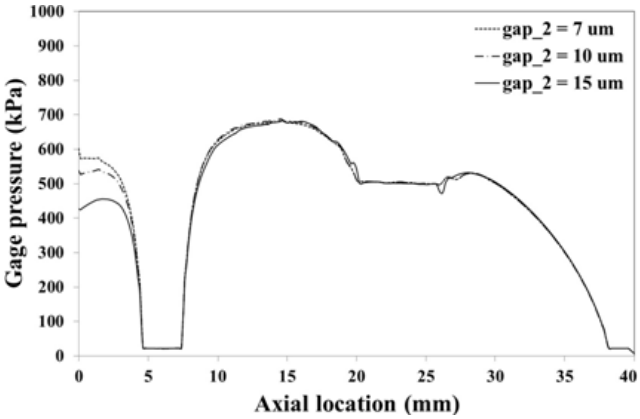

(b) Rotating speed = 60000 rpm

Fig. 5 With a rotating speed of 15000 rpm and 60000 rpm respectively, the pressure distributed along axial line 1 in air gap 1 between the spindle and the journal bearing was illustrated.

With a rotating speed of 15000 rpm, 30000 rpm and 60000 rpm respectively, the pressure in air gaps 2 and 3 were analyzed when these two air gaps were under the conditions shown in Fig. 4. The pressure distribution in air gap 1 between the spindle and the journal bearing was displayed in Fig. 5. In Fig. 5, the length of the axial line 1 was 40 mm. The gage pressure was 0 at the location of the air outlet. When the vertical milling was at the initial stage (i.e., the feeding process), the axial force pushed air gap 2 to a thickness of 7 μm. The thickness of gap 3 became 13 μm. When the spindle rotated at 15000 rpm, the pressure in air gap 1 along axial line 1 was the highest among the three

conditions, namely, the feeding, the stable cutting and the retracting stages. In Fig. 5, it was seen the two curves had a horizontal segment of 6 mm in length superimposed. With a gage pressure around 400 kPa, that horizontal segment was just the location of the air inlet of the porous insert below the journal bearing. The faster the rotating speed, the higher the pressure in air gap 1 would be. Thus, the axial pressure distribution curves changed. When the rotating speed was 60000 rpm, as shown in Fig. 5(b), the pressure in air gap 1 increased significantly to a level above 600 kPa in the zone between the air inlet and the air outlet (see Fig. 3(a)). It was noted the pressure distribution was almost not affected by change of thickness of air gap 2, except in the zone between the axial locations of 0 mm and 5 mm where the pressure increased as the thickness of air gap 2 reduced from 15 μm to 7 μm.

Table 1 The average pressure on the surface of spindle below air gap 1.

Rotating Speed (rpm)	Average Pressure on the Spindle Surface below Air Gap 1 (kPa)		
	Gap 2 = 7 μm Gap 3 = 13 μm	Gap 2 = 10 μm Gap 3 = 10 μm	Gap 2 = 15 μm Gap 3 = 5 μm
15,000	274.8	272.4	264.6
30,000	301.0	300.5	293.2
60,000	382.7	380.4	376.7

Table 2 The stiffness of spindle under various gap thicknesses of thrust bearing and rotating speeds.

Rotating Speed (rpm)	Stiffness of Spindle (N/μm)		
	Gap 2 = 7 μm Gap 3 = 13 μm	Gap 2 = 10 μm Gap 3 = 10 μm	Gap 2 = 15 μm Gap 3 = 5 μm
15,000	64.6	56. 5	49.3
30,000	94.8	90.3	84.1
60,000	122.3	121.2	119.1

Under various gap thicknesses of the thrust bearing and rotating speeds, the average pressure on the part of the spindle surface located below air gap 1 was shown in Table 1. The stiffness of the spindle was listed in Table 2. From Table 1, it was seen that the average pressure on the part of the spindle surface below air gap 1 and the stiffness of the spindle were only slightly affected by change in thickness of the air gap of the thrust bearing. During cutting, the feeding process reduced the thickness of air gap 2 and maximized the average pressure on the spindle surface and the stiffness of the spindle. During the retracting process, the gravitational force increased the thickness of air gap 2 and minimized the average pressure on the spindle surface and the stiffness of the spindle. The faster the rotating speed, the higher the pressure on the surface of spindle and the stiffness of spindle.

Variation of pressure in the air gaps between the spindle and the thrust bearing

In analysis, it was assumed the axial component of the cutting force during feeding of the vertical milling machine reduced the thickness of air gap 2 between the spindle flange and the rear thrust plate to 7 μm, while increased the thickness of air gap 3 between the spindle flange and the front thrust plate to 13 μm. During retracting process, due to the dead weight of the spindle module, the thickness of air gap 2 was increased to 15 μm, while the thickness of air gap 3 was decreased to 5 μm. When the thickness of air gap 2 was 7 μm, 10 μm and 15 μm individually, the pressure distributed along radial line 3 in air gap 3 was illustrated in Fig. 6(a) and Fig. 6(b) for a rotating speed of 15000 rpm and 60000 rpm respectively. While the pressure distributed along radial line 2 in air gap 2 was illustrated in Fig. 7(a) and Fig. 7 (b) for a rotating speed of 15000 rpm and 60000 rpm respectively.

From Fig. 6, it was noticed that, during the feeding process in cutting, the thickness of air gap 2 was compressed to 7 μm and the thickness of air gap 3 was increased to 13 μm. Under this condition, the pressure distributed along radial line 3 was the lowest. During the retracting process, the thickness of air gap 2 was increased to 15 μm and the thickness of air gap 3 was reduced to 5 μm. At this stage, the pressure distributed along radial line 3 was the highest. From Fig. 7, it was also noticed that, in feeding, when the thickness of air gap 2 was reduced to 7 μm, the pressure distributed along radial line 2 was the highest. In retracting, when the thickness of air gap 2 was increased to 15 μm, the pressure distributed along radial line 2 was the lowest.

Fig 6(a) and Fig. 7(a) showed, when the rotating speed was 15000 rpm, there was a nearly horizontal line segment with a length of 6 mm in every pressure distribution curve. That indicated the location of the air inlet of the porous insert on the thrust bearing. The gauge pressure there was the

highest in the pressure distribution curves which illustrated the pressure distributed along radial lines 2 and 3 in air gaps 2 and 3, respectively. During feeding, when the thickness of air gap 2 was reduced to 7 μm, the pressure at the air inlet of the porous insert in air gap 2 was about 400 kPa. In Fig. 3, it was seen both ends of radial line 2 were next to air outlets. Thus, the gauge pressure at both ends of air gap 2 dropped to zero. During retracting, when the thickness of air gap 2 was increased to 15 μm, the pressure along the 6 mm-long air inlet of the porous insert in air gap 2 was still 400 kPa. Regarding air gap 2, the air was released at the edge of the thrust plate so that the gap pressure over there dropped to zero gauge pressure. However, the pressure in air gap 2 from the porous insert on thrust plate to air gap 1 of the journal bearing only decreased slightly. When the rotating speed was increased to 60000 rpm, the pressure along radial line 2 in air gap 2 went up and the pressure distribution changed. The same situation happened to the pressure along radial line 3 in air gap 3.

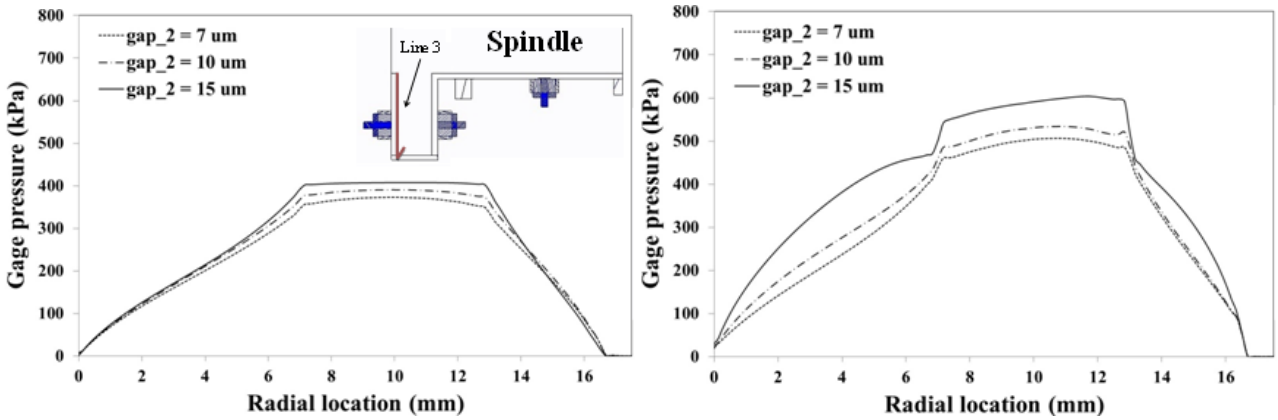

(a) Rotating speed = 15000 rpm (b) Rotating speed = 60000 rpm

Fig. 6 The pressure distributed along radial line 3 in air gap 3 as thickness of air gap 2 was 7 μm, 10 μm and 15 μm respectively.

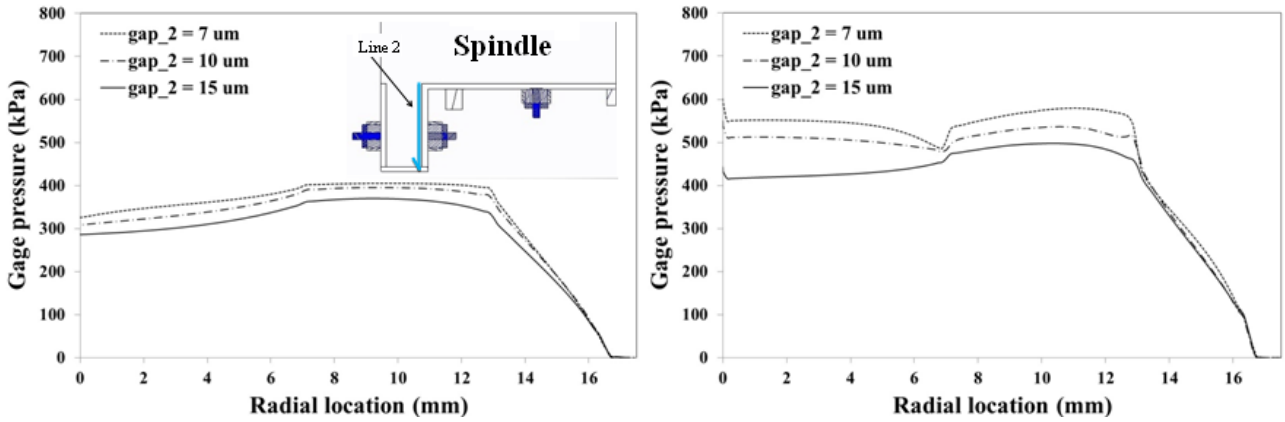

(a) Rotating speed = 15000 rpm (b) Rotating speed = 60000 rpm

Fig. 7 The pressure distributed along radial line 2 in air gap 2 as thickness of air gap 2 was 7 μm, 10 μm and 15 μm respectively.

With an eccentricity ratio of 0.3, under different rotating speeds and various gap thicknesses of the thrust bearing, the average pressure on the front surface of the spindle flange located in air gap 3 was listed in Table 3; the average pressure on the rear surface of the spindle flange located in air gap 2 was listed in Table 4. Table 3 revealed that, during feeding, the increased thickness of air gap 3 between the front thrust plate and the spindle flange resulted in pressure reduction on the front surface of the spindle flange. Table 4 showed that, during retracting, the increased thickness of air gap 2 between the rear thrust plate and the spindle flange resulted in pressure reduction on the rear surface of the spindle flange. Table 5 showed the net force applied on the spindle flange which was the sum of the forces subjected to the front and the rear surfaces of the spindle flange in air gap 3 and air gap 2 respectively. The vertically downward direction was defined as the +Z direction. The upward net

force applied on the spindle flange during feeding was the resultant of upward cutting force and downward gravitational force. The downward net force applied on the spindle flange during retracting was due to the weight of the spindle module.

Table 3 The average pressure on the front surface of the spindle flange located in air gap 3.

Spindle Speed (rpm)	Average Pressure on Front Surface of Spindle Flange in Air Gap 3 (kPa)		
	Gap 2 = 7 μm Gap 3 = 13 μm	Gap 2 = 10 μm Gap 3 = 10 μm	Gap 2 = 15 μm Gap 3 = 5 μm
15,000	139.2	158.8	212.5
30,000	171.8	202.4	270.7
60,000	279.0	326.4	412.1

Table 4 The average pressure on the rear surface of the spindle flange located in air gap 2.

Rotating Speed (rpm)	Average Pressure on Rear Surface of Spindle Flange in Air Gap 2 (kPa)		
	Gap 2 = 7 μm Gap 3 = 13 μm	Gap 2 = 10 μm Gap 3 = 10 μm	Gap 2 = 15 μm Gap 3 = 5 μm
15,000	253.5	232.9	205.8
30,000	305.8	277.3	236.1
60,000	447.9	409.5	345.4

Table 5 The net force applied on the spindle flange.

Rotating Speed (rpm)	Net Force on the Spindle Flange (N)		
	Gap 2 = 7 μm Gap 3 = 13 μm	Gap 2 = 10 μm Gap 3 = 10 μm	Gap 2 = 15 μm Gap 3 = 5 μm
15,000	481	312	-31
30,000	547	302	-152
60,000	622	296	-286

Remark: Positive net force means the force points downward along +Z axis; negative net force means the force points upward along -Z axis.

Concluding remarks

The analytical results indicated that, during cutting of the vertical milling machine, the radial component of the cutting force subjected to the thrust bearing was very small. Therefore, only the axial component of the cutting force was considered to be applied to the thrust bearing. The average pressure on the surface of spindle below the air gap 1 and the stiffness of spindle were not significantly affected by the changes of gap thicknesses of the thrust bearing.

During feeding process in cutting, the increased thickness of air gap 3 between the front thrust plate and the spindle flange resulted in pressure reduction on the front surface of the spindle flange. The net force on the spindle flange pointed downward along +Z axis. During retracting process, the increased thickness of air gap 2 between the rear thrust plate and the spindle flange resulted in pressure reduction on the rear surface of the spindle flange. The net force on the spindle flange pointed upward along -Z axis. The net force on the spindle flange during feeding was much larger than that during retracting, especially in lower rotating speed.

References

[1] M. Szwarcman, R. Gorez: Int. J. Mach Tool Design and Research, Vol. 18 (1978), p. 49

[2] H. Rao: *Simulation based on FLUENT and experimental research of porous aerostatic bearing*, Master Thesis, Harbin Institute of Technology, China (2006)

[3] J.M. Wang: *A study on part of key techniques in ultra-precision aerostatic bearing axes system*, Ph.D. Thesis, National University of Defense Technology, China (2007)

[4] T.Y. Huang, B.Z.Wang, S.C. Lin and S.Y. Hsu: Key Engineering Materials Vol. 625 (2014), p. 384